On the Structural Dichotomy of Cationic, Anionic, and Neutral FeS_2

Detlef Schröder,* Ilona Kretzschmar, and Helmut Schwarz

Institut für Organische Chemie der Technischen Universität Berlin, Strasse des 17. Juni 135, D-10623 Berlin, Germany

Chad Rue and P. B. Armentrout*

Department of Chemistry, University of Utah, Salt Lake City, Utah 84112

Received February 26, 1999

Structural and thermochemical aspects of the FeS_2^+ cation are examined by different mass spectrometric methods and ab initio calculations using density functional theory. Accurate threshold measurements provide thermochemical data for FeS^+, FeS_2^+, and $FeCS^+$, i.e., $D_0(Fe^+-S) = 3.06 \pm 0.06$ eV, $D_0(SFe^+-S) = 3.59 \pm 0.12$ eV, $D_0(Fe^+-S_2) = 2.31 \pm 0.12$ eV, and $D_0(Fe^+-CS) = 2.40 \pm 0.12$ eV. Fortunate circumstances allow a refinement of the data for FeS^+ by means of ion/molecule equilibria, and the resulting $D_0(Fe^+-S) = 3.08 \pm 0.04$ eV is among the most precisely known binding energies of transition-metal compounds. The present results agree with previous experimental findings and also corroborate the computed data for FeS^+ and FeS_2^+. Ab initio calculations predict a sextet ground state ($^6A_1$) for FeS_2^+ with a cyclic structure. The presence of S−S and Fe−S bonds accounts for the fact that not only reactions involving the disulfur unit but also sulfur-atom transfer can occur. In contrast, the FeS_2^- anion is an acyclic iron disulfide. In the gas phase, neutral FeS_2 may adopt either acyclic or cyclic structures, which are rather close in energy according to the calculations.

1. Introduction

Iron sulfides are among the most important ores of this metal, and binary Fe/S and heterometallic clusters have important functions in biochemistry. In fact, iron sulfide has even been postulated to have played a key role in the evolution of life.[1,2] A marked difference in comparison to the related metal oxides is the tendency of sulfur to form reasonably strong S−S bonds, e.g., the disulfide unit in pyrite.

Previous work concerning neutral and charged FeS_2 includes ion/molecule reactions[3,4] and spectroscopic studies.[3−5] Here, we report a combined mass-spectrometric/ab initio study of the FeS_2^+ cation along with some complementary data for the neutral and anionic species. By analogy with the previously reported FeO_2 system,[6] our main interest concerns the structural dichotomy of FeS_2, which can correspond to either the cyclic form **I**, denoted as $Fe(S_2)$, or the acyclic iron disulfide **II**, denoted as SFeS (Scheme 1). In the present context, the formula FeS_2 shall not imply any structural assignments.

2. Experimental and Theoretical Procedures

Three different mass spectrometric techniques are used in this study. As the experimental details have been described elsewhere, neither all raw data nor the data analysis are described explicitly. For further details we refer to the literature sources given below as well as the Supporting Information available on the Internet.

Scheme 1

I II

2.1. Guided-Ion Beam (GIB). Thermochemical thresholds associated with the reactions of Fe^+ and FeS^+ with carbon disulfide are determined using a GIB mass spectrometer.[7,8] Briefly, Fe^+ is formed by Ar^+-sputtering from an iron cathode near the beginning of a meter-long flow tube containing ca. 1 Torr of helium and argon, which collisionally thermalize the ions. If desired, Fe^+ is converted to FeS^+ by adding a small amount of COS to the flow gases. The ions of interest are then mass-selected with a magnet and directed into an octopole ion guide which passes through a collision cell. The ions travel through the octopole at well-defined collision energies ranging from 0 to 100 eV, while carbon disulfide is present in the cell at pressures of 0.05−0.1 mTorr. The reactant and product ions are then mass-analyzed by a quadrupole mass filter and detected. Well-documented routines[7−10] are applied for the conversion of the raw data into product cross sections as functions of the center-of-mass energies as well as the subsequent analysis to extract thermochemical thresholds at 0 K.

2.2. Ion-Cyclotron Resonance (ICR). Ion−molecule reactions at thermal energies are studied using a Spectrospin CMS 47X FTICR

(1) Williams, R. J. P. *Nature* **1990**, *343*, 213.
(2) Drobner, E.; Huber, H.; Wächtershäuser, G.; Stetter, K. O. *Nature* **1990**, *346*, 742.
(3) McMahon, T. J.; Jackson, T. C.; Freiser, B. S. *J. Am. Chem. Soc.* **1989**, *111*, 421.
(4) Nakajima, A.; Hayase, T.; Hayakawa, F.; Koya, K. *Chem. Phys. Lett.* **1997**, *280*, 381.
(5) Zhang, N.; Hayase, T.; Kawamata, H.; Nakao, K.; Nakajima, A.; Kaya, K. *J. Chem. Phys.* **1996**, *104*, 3413.
(6) Schröder, D.; Fiedler, A.; Schwarz, J.; Schwarz, H. *Inorg. Chem.* **1994**, *33*, 5094.
(7) Ervin, K. M.; Armentrout, P. B. *J. Chem. Phys.* **1985**, *83*, 166.
(8) Schultz, R. H.; Armentrout, P. B. *Int. J. Mass Spectrom. Ion Processes* **1991**, *107*, 29.
(9) Schultz, R. H.; Crellin, K. C.; Armentrout, P. B. *J. Am. Chem. Soc.* **1991**, *113*, 8590.
(10) Armentrout, P. B. In *Advances in Gas-Phase Ion Chemistry*; Adams, N. G., Babock, L. M., Eds.; JAI Press: Greenwich, 1992; Vol. 1, p 83.

10.1021/ic990241b CCC: $18.00
Published on Web 06/30/1999

mass spectrometer.[11] In brief, FeS^+ is generated by reacting mass-selected $^{56}Fe^+$ with carbonyl sulfide. Unlike ethylene sulfide,[3] COS reacts with bare Fe^+ about 2 orders of magnitude faster than with FeS^+, thus providing good yields of FeS^+. For the generation of FeS_2^+ ethylene sulfide is used.[3] Subsequent thermalization is achieved by pulsing in argon, which is pumped off prior to reactivity measurements. Reagent gases are introduced to the FTICR cell either via leak or pulsed valves. In the equilibrium measurements (see below), Fe^+ and FeS^+ ions are allowed to interact with CO and/or COS at various pressures and reaction times. Partial pressures of the neutrals are measured with a calibrated[12] ion gauge (IMG070, Balzers, Lichtenstein) and corrected for relative sensitivities.[13] Equilibria are considered to be established if the Fe^+/FeS^+ ratios are more or less independent of reaction time.[14,15] Fortunately, secondary reactions do not disturb the equilibrium measurements with Fe^+ and FeS^+ in the presence of CO and COS[15] because association reactions as well as formation of FeS_2^+ are slow compared to equilibration.[16]

2.3. Sector-Field Mass Spectrometry. These experiments are performed with a modified VG ZAB/HF/AMD 604 four-sector mass spectrometer[17] of BEBE configuration (B stands for magnetic and E for electric sector). FeS_2^+ and FeS_2^- are generated by chemical ionization (CI) of a mixture of $Fe(CO)_5$ and ethylene sulfide using carbon monoxide as a supporting CI gas. FeS_2^- is always accompanied by small amounts of FeO_4^- due to air leaking into the ion source.[6] While the mass difference between these ions was too small to be resolved, the mass spectra of FeS_2^- are corrected for interfering FeO_4^- on the basis of the abundance of the FeO fragments.[6] The ions of interest are accelerated to 8 keV kinetic energy, mass-selected using B(1)/E(1), and then subjected to the following experiments:[17,18] (i) collisional activation (CA) of FeS_2^+ using helium as collision gas; (ii) neutralization reionization ($^+NR^+$) of FeS_2^+ via neutrals to cations using xenon and oxygen, respectively; (iii) charge reversal ($^-CR^+$) of FeS_2^- to cationic species using oxygen as collision gas; (iv) neutralization reionization ($^-NR^+$) of FeS_2^- to cations using oxygen in both collisions; and (v) collisional activation of FeS_2^+ made by charge reversal of FeS_2^- ($^-CR^+/CA$).

2.4. Ab Initio Calculations. Neutral and charged FeS_2 are studied computationally at the B3LYP level of theory using Gaussian94[19] in conjunction with the standard 6-311+G* basis sets. In all cases, full geometry optimizations are performed and the nature of the stationary points (minima, first- or higher-order saddle points) is evaluated by frequency calculations.[20] These properties are further used to calculate thermal corrections for ΔH and ΔG (298 → 0 K), applying standard routines implemented in Gaussian94. For the quartet and sextet manifolds of the FeS_2^+ cation, all possible orbital states are considered in optimizations at the B3LYP/6-311+G* level of theory, but even upon deliberate orbital switching not all symmetries converge at this level. In the calculations of the doublet state of FeS_2^+, neutral FeS_2, and FeS_2^- anion, only the different spin multiplicities (see below) are optimized with B3LYP/6-311+G*; low-lying states of other symmetries may exist as well. Further, our computations with B3LYP should only be regarded as a first-order approach because this level of theory cannot treat excited electronic states very accurately, and some of the wave functions are contaminated by higher-order spin states.

3. Results

Our main interest concerns the elucidation of the connectivity of FeS_2 in its various charge states. However, let us first consider some properties of diatomic FeS^+ in more detail, because its thermochemistry is used as an input parameter in our assessment of the FeS_2 species. The section on FeS^+ is followed by descriptions of the experimental and theoretical results for FeS_2^+ along with complementary results for the neutral and anionic species.

3.1. Thermochemistry of FeS^+ Cation. The redox chemistry of neutral and charged FeS in the gas phase is quite well established.[21] The electron affinity EA(FeS) = 1.76 ± 0.10 eV was determined by photoelectron spectroscopy,[5] and an ionization energy IE(FeS) = 8.3 ± 0.3 eV was derived from bracketing experiments.[21] Combined with the heat of formation of the neutral, $\Delta_f H$(FeS) = 3.82 ± 0.15 eV,[22] these results imply bond dissociation energies of $D_0(Fe-S^-)$ = 2.99 ± 0.18 eV for the anion, $D_0(Fe-S)$ = 3.31 ± 0.15 eV for neutral FeS, and $D_0(Fe^+-S)$ = 2.91 ± 0.34 eV for the monocation. Note also that $D_0(Fe^{2+}-S)$ = 2.6 ± 0.7 eV for the dication is known.[21] Previous, direct measurements of $D_{298}(Fe^+-S)$ gave values of 2.65 ± 0.26 eV[3] and 2.82 ± 0.22 eV,[23] which are converted to $D_0(Fe^+-S)$ = 2.68 ± 0.26 eV and 2.85 ± 0.22 eV by use of the thermal corrections calculated at the B3LYP/6-311+G* level of theory. An ab initio value of 2.83 eV[21] is in keeping with these figures. As an average, we conservatively conclude that $D_0(Fe^+-S)$ = 2.82 ± 0.45 eV. Because FeS^+ is used as a precursor in the formation of FeS_2^+ (see below), the error in this value propagates to that for FeS_2^+. To circumvent this problem, we refined the thermochemistry of FeS^+ by combining guided-ion beam (GIB) and ion-cyclotron resonance (ICR) mass spectrometry.

$$Fe^+ + CS_2 \rightarrow FeS^+ + CS \quad (1)$$

$$Fe^+ + CS_2 \rightarrow FeCS^+ + S \quad (2)$$

Under GIB conditions, Fe^+ reacts endothermically with CS_2 to yield FeS^+ and $FeCS^+$ according to reactions 1 and 2, along with some charge-transfer formation of CS_2^+ at elevated energies (Figure 1). Analysis of these data yields measured thresholds of 1.44 ± 0.05 and 2.35 ± 0.12 eV for the FeS^+ and $FeCS^+$ products, respectively.[24] These reaction thresholds correspond to $D_0(Fe^+-S)$ = 3.06 ± 0.06 eV and $D_0(Fe^+-CS)$ = 2.15 ± 0.13 eV, respectively. Our experimental value of $D_0(Fe^+-S)$ is toward the upper range of the error margins of the previous results. Note that a barrier in excess of the endother-

(11) Eller, K.; Schwarz, H. *Int. J. Mass Spectrom. Ion Processes* **1989**, *93*, 243.
(12) Schröder, D.; Schwarz, H.; Clemmer, D. E.; Chen, Y.-M.; Armentrout, P. B.; Baranov, V. I.; Böhme, D. K. *Int. J. Mass Spectrom. Ion Processes* **1997**, *161*, 177.
(13) Bartmess, J. E.; Georgiadis, R. M. *Vacuum* **1983**, *33*, 149.
(14) Dieterle, M.; Harvey, J. N.; Schröder, D.; Schwarz, J.; Heinemann, C.; Schwarz, H. *Chem. Phys. Lett.* **1997**, *277*, 399.
(15) Schröder, D.; Schwarz, H.; Hrušák, J.; Pyykkö, P. *Inorg. Chem.* **1998**, *37*, 624.
(16) For further details, see the Supporting Information.
(17) Schalley, C. A.; Schröder, D.; Schwarz, H. *Int. J. Mass Spectrom. Ion Processes* **1996**, *153*, 173.
(18) Schalley, C. A.; Hornung, G.; Schröder, D.; Schwarz, H. *Int. J. Mass Spectrom.* **1998**, *172/173*, 181.
(19) Frisch, M. J.; Trucks, G. W.; Schlegel, H. B.; Gill, P. M. W.; Johnson, B. G.; Robb, M. A.; Cheeseman, J. R.; Keith, T.; Petersson, G. A.; Montgomery, J. A.; Raghavachari, K.; Al-Laham, M. A.; Zakrzewski, V. G.; Ortiz, J. V.; Foresman, J. B.; Peng, C. Y.; Ayala, P. Y.; Chen, W.; Wong, M. W.; Andres, J. L.; Replogle, E. S.; Gomperts, R.; Martin, R. L.; Fox, D. J.; Binkley, J. S.; Defrees, D. J.; Baker, J.; Stewart, J. P.; Head-Gordon, M.; Gonzalez, C.; Pople, J. A. *Gaussian 94*, revision B.3; Gaussian, Inc.: Pittsburgh, PA, 1995.
(20) For a list of the calculated frequencies, see the Supporting Information.
(21) Harvey, J. N.; Heinemann, C.; Fiedler, A.; Schröder, D.; Schwarz, H. *Chem.—Eur. J.* **1996**, *2*, 1230.
(22) Drowart, J.; Pattoret, A.; Smoes, S. *Proc. Br. Ceram. Soc.* **1967**, *8*, 67.
(23) Jackson, T. C.; Freiser, B. S. *Int. J. Mass Spectrom. Ion Processes* **1986**, *72*, 169.
(24) Five independent data sets are analyzed and yield average fitting parameters of σ_0 = 2.5 ± 0.4, E_0 = 1.44 ± 0.05 eV, and n = 1.8 ± 0.1 for the FeS^+ product and σ_0 = 0.56 ± 0.13, E_0 = 2.35 ± 0.12 eV, and n = 2.4 ± 0.2 for the $FeCS^+$ product. Uncertainties in the threshold values include variations in the values for different data sets, for the range of n values, and the absolute uncertainty in the energy scale. Conversion of these thresholds to bond energies utilizes $D_0(SC-S)$ = 4.50 ± 0.04 eV from ref 28.

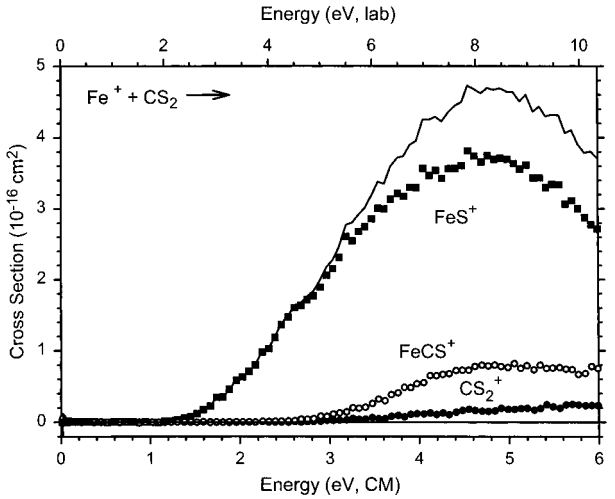

Figure 1. Product cross sections for the reactions of Fe^+ with CS_2 to form FeS^+ (■), $FeCS^+$ (○), and CS_2^+ (●) as a function of center-of-mass energy (lower axis) and laboratory energy (upper axis).

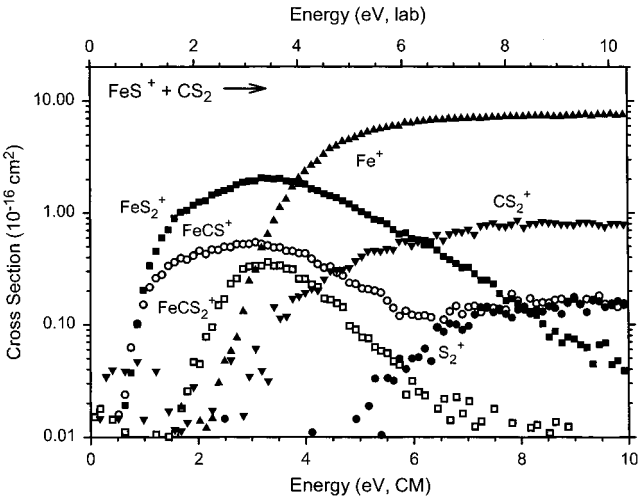

Figure 2. Product cross sections for the reactions of FeS^+ with CS_2 to form $FeCS^+$ (○), FeS_2^+ (■), $FeCS_2^+$ (□), CS_2^+ (▼), Fe^+ (▲), and S_2^+ (●) as a function of center-of-mass energy (lower axis) and laboratory energy (upper axis).

micity of reaction 1 would result in an underestimation of $D_0(Fe^+-S)$ and thus cannot account for the difference.

Fortunate circumstances allow some further improvement in the precision of this bond energy by independent ICR experiments. Thus, sulfur transfer between iron cations and carbonyl sulfide (reaction 3) is reversible under ICR conditions, and neither side reactions nor consecutive processes disturb the corresponding equilibrium measurements.[15]

$$Fe^+ + COS \rightleftarrows FeS^+ + CO \qquad (3)$$

The experimental rate constants are $k_3 = (2.6 \pm 1.1) \times 10^{-10}$ cm^3 molecule^{-1} s^{-1} and $k_{-3} = (0.22 \pm 0.09) \times 10^{-10}$ cm^3 molecule^{-1} s^{-1} for the forward and backward reactions, respectively. Accordingly, the kinetic measurements give an equilibrium constant of $K_{eq} = 11.6 \pm 4.6$. Note that the significant systematic error in the calibration of the absolute rate constants[12] cancels in the determination of K_{eq}. Assuming an effective temperature of 298 ± 50 K in these measurements,[12,14] the Gibbs−Helmholtz equation implies $\Delta_r G(298\ K) = -0.063 \pm 0.014$ eV for reaction 3. Further, it is possible to establish equilibria between Fe^+ and FeS^+ at different pressures of COS and CO.[15] As an average of three independent equilibrium measurements for different COS/CO ratios, we obtain $K_{eq} = 6.1 \pm 0.8$, which translates to $\Delta_r G(298\ K) = -0.046 \pm 0.004$ eV for reaction 3. The reaction free energies determined via the kinetic approach and in the equilibrium measurements are in favorable agreement. Thus, we consider $\Delta_r G(298\ K) = -0.05 \pm 0.03$ eV as a compromise, where the error also includes systematic errors of the ion-gauge sensitivities for CO and COS[13] as well as the estimated uncertainty of the effective temperature. Interestingly, but not uncommonly for reactions involving atomic species,[14,15] B3LYP/6-311+G* calculations indicate a considerable thermal correction of 0.11 ± 0.02 eV in favor of the right side of reaction 3 at room temperature. Conversion to 0 K yields $\Delta_r G(0\ K) = \Delta_r H(0\ K) = 0.06 \pm 0.04$ eV. In other words, formation of FeS^+ is slightly endothermic at 0 K, but becomes exoergic at room temperature due to entropic contributions. The fate of reaction 3 as an entropy-driven process makes sense, as two vibrations in the COS reactant become rotations in the diatomic products. Together with $D_0(OC-S) = 3.140 \pm 0.005$ eV,[25,26] this result leads to $D_0(Fe^+-S) = 3.08 \pm 0.04$ eV, which is in excellent agreement with the GIB experiments. The consistency of the values for $D_0(Fe^+-S)$ determined with two different experimental techniques is remarkable considering that both methods have no parameters in common except the atomic data.

3.2. Thermochemistry and Reactivity of FeS_2^+. A previous investigation of FeS_n^+ cations ($n = 1-6$) by McMahon et al.[3] reported $D_{298}(SFe^+-S) = 3.82 \pm 0.35$ eV and $D_{298}(Fe^+-S_2) = 2.08 \pm 0.22$ eV for FeS_2^+ species formed by sequential S-atom transfer from ethylene sulfide to Fe^+ cation. These values correspond to $D_0(SFe^+-S) = 3.85 \pm 0.35$ eV and $D_0(Fe^+-S_2) = 2.11 \pm 0.22$ eV after thermal correction. Further, the reactivity of FeS_2^+ led these authors to conclude that structure **I**, i.e., $Fe(S_2)^+$ with an S−S bond, is preferred.

Reaction of FeS^+ with CS_2 under GIB conditions (Figure 2) gives $FeCS^+$ and FeS_2^+ at low energies along with Fe^+ at higher energies as the major products. A significant fraction of charge transfer to yield CS_2^+ along with minor amounts of $FeCS_2^+$ and S_2^+ appears at elevated kinetic energies and is not pursued further.[27] Formation of the three major products at low energies can be ascribed to the occurrence of reactions 4−6.

$$FeS^+ + CS_2 \rightarrow \begin{cases} FeCS^+ + S_2 & (4) \\ FeS_2^+ + CS & (5) \\ Fe^+ + [C,S_3] & (6) \end{cases}$$

Analysis of the individual product cross sections gives thresholds of 0.82 ± 0.11 eV for $FeCS^+$, 0.91 ± 0.10 eV for FeS_2^+, and 2.86 ± 0.12 eV for Fe^+. Formation of $FeCS^+$ at a threshold less than 1 eV can only be rationalized if an S_2 molecule is generated, because formation of two sulfur atoms is much more endothermic. Reaction 5 is directly analogous to reaction 1 and must correspond to loss of intact CS. Formation of Fe^+ in reaction 6 is less obvious as it may be associated

(25) Pedley, J. B.; Naylor, R. D.; Kirby, S. P. *Thermochemical Data of Organic Compounds*; Chapman and Hall: London, 1986. Corrected to 0 K using $H°-H°$ (298.15) values taken from ref 26.
(26) Chase, M. W., Jr.; Davies, C. A.; Downey, J. R., Jr.; Frurip, D. J.; McDonald, R. A.; Syverud, A. N. *J. Phys. Chem. Ref. Data* **1985**, *14*, Suppl. 1 (JANAF Tables).
(27) Capron, L.; Feng, W. Y.; Lifshitz, C.; Tjelta, B. L.; Armentrout, P. B. *J. Phys. Chem.* **1996**, *100*, 16571.

with either $CS_2 + S$, $CS + S_2$, or a putative CS_3 species as neutral products (reactions 6a−c). Reaction 6a corresponds to

$$FeS^+ + CS_2 \rightarrow \begin{cases} Fe^+ + CS_2 + S & (6a) \\ Fe^+ + CS + S_2 & (6b) \\ Fe^+ + CS_3 & (6c) \end{cases}$$

simple collision-induced dissociation (CID) of FeS^+, having a minimal energy requirement of $D_0(Fe^+-S) = 3.08 \pm 0.04$ eV (see above). Moreover, previous studies of transition-metal sulfides[28] suggest that CS_2 is not an efficient target gas for CID and the threshold is expected to significantly exceed $D_0(Fe^+-S)$. Therefore, reaction 6a is unlikely to occur at 2.86 ± 0.12 eV, although it may contribute to the cross section at higher energies. Likewise, reaction 6b cannot account for the threshold of the Fe^+ channel because the corresponding neutrals are even less stable than $CS_2 + S$. However, this reaction also must occur at higher energies as the cross sections for $FeCS^+$ and FeS_2^+ decline at energies roughly corresponding to their dissociation to the Fe^+ product. Thus, at threshold, formation of intact CS_3 as a stable neutral[29] must be involved (reaction 6c). Ab initio calculations by Froese and Goddard[30] determined that a cyclic CS_3 isomer, i.e., thiodithiiranone, is 0.46 eV more stable than $CS_2 + S$. Thus, neutral CS_3 can indeed account for the observed threshold of reaction 6 being lower in energy than the CID process, reaction 6a. However, the limited size of the basis sets used in the quoted theoretical study (6-31G*) does not allow a good quantitative comparison between experiment and theory. If we assume that reaction 6c does not involve a barrier in excess of the reaction endothermicity, the experimental threshold of the Fe^+ channel suggests $D_0(S-CS_2) = 0.22 \pm 0.14$ eV or $\Delta_f H(0\ K) = 3.83 \pm 0.14$ eV for the cyclic CS_3 species.

The experimentally determined threshold for formation of $FeCS^+$ in reaction 4 implies $D_0(Fe^+-CS) = 2.40 \pm 0.12$ eV, which is somewhat above $D_0(Fe^+-CS) = 2.15 \pm 0.13$ eV obtained from reaction 2. The difference is attributed to the fact that, for the Fe^+/CS_2 couple, sulfur transfer (reaction 1) competes efficiently and may somewhat suppress the $FeCS^+$ channel, thereby causing a slightly delayed threshold for reaction 2. For the FeS^+/CS_2 couple, however, the $FeCS^+$ and FeS_2^+ products have comparable cross sections at low energies (Figure 2) suggesting that $D_0(Fe^+-CS) = 2.40 \pm 0.12$ eV derived from reaction 4 is more accurate. Both values are consistent with a lower bound of $D(Fe^+-CS) > 2.08 \pm 0.22$ eV suggested earlier.[31]

The threshold for FeS_2^+ formation transforms to $D_0(SFe^+-S) = 3.59 \pm 0.12$ eV or $D_0(Fe^+-S_2) = 2.31 \pm 0.12$ eV. Within the error margins, the latter value agrees with $D_0(Fe^+-S_2) = 2.11 \pm 0.22$ eV derived using photodissociation (reaction 7) and ligand-exchange processes (reaction 8).[3] The value for $D_{298}(SFe^+-S)$ derived in the same study, which converts to $D_0(SFe^+-S) = 3.82 \pm 0.35$ eV, differs from ours partly as a consequence of our revision of $D_0(Fe^+-S)$.

$$FeS_2^+ + h\nu \rightarrow Fe^+ + S_2 \quad (7)$$

$$FeS_2^+ + L \rightarrow FeL^+ + S_2 \quad (8)$$

We briefly revisited the ligand-exchange experiments (reaction 8) and could confirm ligand exchange with L = benzene as reported in ref 3. Some recent revision of $D_0(Fe^+-C_6H_6)$ which is used as an anchor in ref 3 implies an upper bound of $D_0(Fe^+-S_2) \leq D_0(Fe^+-C_6H_6) = 2.15 \pm 0.10$ eV.[32] A lower bound of $D_0(Fe^+-S_2)$ can be derived from the FeS_2^+/1,3-butadiene couple (reaction 9). The overall rate constant amounts to $k_9 = (4.3 \pm 0.9) \times 10^{-10}$ cm^3 molecule^{-1} s^{-1} compared to a collision rate of 11.3×10^{-10} cm^3 molecule^{-1} s^{-1}.

$$FeS_2^+ + C_4H_6 \rightarrow FeC_4H_4S^+ + H_2S \quad (9)$$

The absence of $FeC_4H_6^+$ according to reaction 8 with L = C_4H_6 as a primary reaction product implies $D_0(Fe^+-S_2) \geq D_0(Fe^+-C_4H_6) = 1.89 \pm 0.11$ eV[33] assuming that ligand exchange is not observed because it is endothermic. $FeC_4H_6^+$ is, however, formed as a secondary reaction product stemming from the $FeC_4H_4S^+$ species formed in reaction 9. This observation is consistent with the generation of an Fe^+−thiophene complex[31] in reaction 9 followed by ligand exchange with excess 1,3-butadiene. As an average of the bracketing experiments, we arrive at $D_0(Fe^+-S_2) = 2.02 \pm 0.24$ eV, which is in agreement with the values reported above.

Note the dual character exhibited by the FeS_2^+ cation in the ion/molecule reactions. Thus, ligand exchange with benzene is in accord with the presence of an S−S bond, i.e., structure **I**, as suggested by McMahon et al.[3] In marked contrast, reaction 9 can be considered a redox process leading to a product without an S−S bond, a process that would be typical for structure **II**. Unlike the authors' arguments in ref 3, which were later adopted by others,[5] we dispute that the thermochemical properties of the FeS_2^+ cation allow any structural distinction of $Fe(S_2)^+$ and $SFeS^+$. In fact, even if structure **II** would be the most stable species, it may well behave like **I** if the interconversion **II** → **I** is facile. For example, low-energy CID as well as threshold photodissociation[3] of FeS_2^+ yields $Fe^+ + S_2$ because this channel is energetically preferred over $FeS^+ + S$ by 1.28 ± 0.04 eV. It is precisely this dichotomy between structures **I** and **II** that has previously been found for the analogous FeO_2^+ system.[6]

The reactivity of the FeS_2^+ cation toward substituted arenes is also examined briefly in order to obtain an estimate of the range of IE(FeS_2). Among several other products formed, electron transfer from the substrate to FeS_2^+ is observed as a major process for 1,4-dimethoxybenzene (IE = 7.53 eV[34]) and as a minor pathway for aniline (IE = 7.72 eV[34]) and is absent with 1,4-dimethylbenzene (IE = 8.44 eV[34]). Further refinement is not attempted because ligand exchange according to reaction 8 competes for all arene ligands studied. Nevertheless, we may conclude from these data that the IE of FeS_2 is similar to that of aniline (7.72 eV) within ±0.5 eV.

As a possibly more direct monitor for the connectivity, let us briefly discuss the results obtained using sector-field mass spectrometry. Here, mass-selected FeS_2^+ and FeS_2^- ions are collided with quasi-stationary target gases at keV kinetic energies, such that highly endothermic direct bond ruptures and electron-transfer processes can occur. Indeed, the CA spectrum of FeS_2^+ (Table 1) shows the FeS^+ fragment as the base peak, while low-energy CID yields Fe^+ with large preference.[3] Loss of atomic sulfur can, however, occur from either $Fe(S_2)^+$ or

(28) Kretzschmar, I.; Schröder, D.; Schwarz, H.; Rue, C.; Armentrout, P. B. *J. Phys. Chem. A* **1998**, *102*, 10060.
(29) Sülzle, D.; Eggsgaard, H.; Carlsen, L.; Schwarz, H. *J. Am. Chem. Soc.* **1990**, *112*, 3750.
(30) Froese, R. D. J.; Goddard, J. D. *J. Chem. Phys.* **1992**, *96*, 7449.
(31) Bakhtiar, R.; Jacobson, D. B. *J. Am. Soc. Mass Spectrom.* **1996**, *7*, 938.
(32) Meyer, F.; Khan, F. A.; Armentrout, P. B. *J. Am. Chem. Soc.* **1995**, *117*, 9740.
(33) Schröder, D.; Schwarz, H. *J. Organomet. Chem.* **1995**, *504*, 123.
(34) Lias, S. G.; Bartmess, J. E.; Liebman, J. F.; Holmes, J. L.; Levin, R. D.; Mallard, W. G. *J. Phys. Chem. Ref. Data* **1988**, *17*, Suppl. 1.

Table 1. Products[a] Observed in the Mass Spectra of $FeS_2^{+/-}$ Ions in the Sector Instrument

	FeS_2^+	FeS^+	S_2^+	Fe^+	S^+
CA	*b*	100	5	85	<1
$^+NR^+$	25	20	100	65	10
$^-CR^+$ [c,d]	25	100	3	40	2
$^-NR^+$ [c,d]	90	95	25	100	10
$^-CR^+$/CA	*b*	100	*e*	95	*e*

[a] Intensities given relative to the base peak, 100%. [b] This entry refers to the precursor cation. [c] The intensities are corrected for interfering FeO_4^-, see Experimental and Theoretical Procedures. [d] Quantitative analysis of the $^-CR^+$ and $^-NR^+$ spectra in terms of the NIDD scheme results in differential intensities of +0.13 (FeS_2^+), −0.29 (FeS^+), +0.06 (S_2^+), +0.08 (FeS_2^+), and +0.02 (S^+); see ref 18 for details of the method. [e] Within the signal-to-noise limit of 10%.

$SFeS^+$ and is thus not structurally indicative. A more direct hint toward structure **I** is provided by the intense signal due to S_2^+ in the $^+NR^+$ spectrum of FeS_2^+, which strongly supports the presence of an S−S bond in the cation. As an additional option,[6,17] sector-field mass spectrometry allows the generation of FeS_2^+ by double-electron detachment from FeS_2^-, i.e., either direct two-electron transfer in a charge-reversal ($^-CR^+$) experiment or stepwise single-electron transfer from the anion via the neutral to the cationic species ($^-NR^+$). It is quite certain that the FeS_2^- anion exhibits structure **II**,[5] for example, the substantial electron detachment energy of 3.28 eV can only be understood if the negative charge is located at sulfur.[4] The $^-CR^+$ spectrum of FeS_2^- supports this assignment in that the S_2^+ fragment indicative of structure **I** is of low abundance. Interestingly, the $^-NR^+$ and $^-CR^+$ spectra of FeS_2^- differ greatly. According to the recently introduced NIDD scheme (NIDD = neutral and ion decomposition difference[18]), such differences are indicative of the chemical behavior of the transient neutral species formed. In particular, the S_2^+ fragment is much more abundant in the $^-NR^+$ than in the $^-CR^+$ spectrum, suggesting the occurrence of the isomerization **II** → **I** at the neutral stage. Finally, collisional activation of the FeS_2^+ cation made by charge inversion of FeS_2^- in a $^-CR^+$/CA experiment yields a fragmentation pattern which is identical to the CA spectrum of genuine FeS_2^+, suggesting that both methods lead to the same structure for the cationic species (see below).

3.3. Theoretical Results. Our computations on the FeS_2 system applied the B3LYP approach, which has been shown to describe the thermochemistry of iron compounds reasonably well.[35] At the B3LYP/6-311+G* level of theory (Table 2), the ground state of the cation is predicted to have structure **I**, i.e., $Fe(S_2)^+$ ($^6A_1$) in which the bond length r_{Fe-S} is significantly longer than in diatomic FeS^+, and r_{S-S} is in the typical range of S−S single-bond lengths. In contrast, the computed geometries of the disulfides $SFeS^+$ **II** show shorter Fe−S and much longer S−S bonds. It is obvious from the data given in Table 2 that structure **I** is more stable than **II**, irrespective of orbital symmetry and spin multiplicity. However, the calculated sextet/quartet splittings are rather small for $Fe(S_2)^+$ as well as $SFeS^+$ (0.04 and 0.07 eV, respectively). Considering the uncertainty of the theoretical approach, no definitive assignment of the respective ground states can be made. Nevertheless, the low-lying states exhibit very similar geometries, while the doublet states can be neglected because they are predicted to be much higher in energy for structures **I** and **II**. Further, B3LYP/6-311+G* predicts $D_0(Fe^+-S) = 3.10$ eV, $D_0(SFe^+-S) = 3.33$ eV, and $D_0(Fe^+-S_2) = 2.39$ eV, which compare quite well with the experimental data discussed above. The good agreement for $D_0(Fe^+-S) = 3.10$ eV is fortuitous, however, considering an average accuracy of about 0.2 eV with B3LYP for Fe compounds and some notably larger deviations.[35] Unfortunately, all our attempts to locate transition structures connecting **I** and **II** failed. By reference to the related FeO_2^+ system,[6] we ascribe this failure to a low activation barrier for the sextets in that the potential-energy surface is flat in the vicinity of structure **II**. This conclusion is based on linear scans of the FeS_2^+ potential-energy surface from **I** to **II** and vice versa as well as the low bending modes of $Fe(S_2)^+$ ($^6A_1$) and $SFeS^+$ ($^6A_1$), which are computed as only 303 and 101 cm^{-1}, respectively[20] (Figure 3). As a consequence of the suspected flatness of the potential-energy surface with respect to the bending of structure **II**, the standard routines for the search of transition structures fail. While more sophisticated theoretical methods may be able to

Table 2. Electronic States, Optimized Geometries, and Relative Energies[a] of FeS_2^+ and Relevant Fragments Calculated at the B3LYP/6-311+G* Level of Theory[b,c]

	state	r_{Fe-S}, Å	r_{S-S}, Å	α_{SFeS}, deg	E_{rel}, eV
$Fe(S_2)^+$, **I**	$^6A_1$	2.26	2.08	54.7	0.00
	$^4A_2$	2.27	2.05	53.5	0.04
	$^4B_2$	2.28	2.05	53.5	0.17
	$^6B_2$	2.33	2.04	52.1	0.28
	$^2B_2$	2.28	2.03	52.9	1.54
$SFeS^+$, **II**	$^6A_1$	2.09	3.42	109.7	1.54
	$^4B_1$	2.01	3.19	105.5	1.63
	$^4B_2$	2.09	3.51	114.4	1.67
	$^6A_2$	2.13	3.90	132.8	2.00
	$^6B_1$	2.12	3.31	102.5	2.09
	$^6B_2$	2.13	4.25	175.3	2.74
	$^2A_1$	2.10	3.51	113.0	2.29
$Fe^+ + S_2$	$^6D/^3\Sigma^-$		1.93		2.39
$FeS^+ + S$	$^6\Sigma^+/^3P$	2.06			3.33[d]
$Fe^+ + 2S$	$^6D/^3P$				6.43[d]

[a] Energies at 0 K including ZPVE relative to $Fe(S_2)^+$ ($^6A_1$). [b] All structures described are characterized as minima on the potential-energy surface by bearing only positive eigenvalues and three real vibrational frequencies. [c] *End-on* structures of $Fe(S_2)^+$ were located as stationary points, but exhibit two imaginary bending modes. [d] These values combine to yield a computed $D_0(Fe^+-S)$ of 3.10 eV.

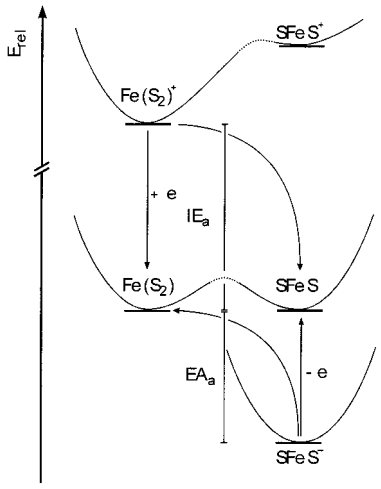

Figure 3. Schematic potential-energy surfaces of anionic, neutral, and cationic FeS_2 showing the dichotomy of structures **I** and **II**. The arrows connecting the $SFeS^-$ anion with the neutral surface indicate the ambiguity in correlating the threshold for electron detachment ($DE_{0\to0}$) from the anion with the adiabatic electron affinity (EA_a) of neutral FeS_2. Similar arrows indicate the uncertainty of correlating the recombination energy of the cation ($RE_{0\to0}$) with the adiabatic IE_a of neutral FeS_2. For relative energies of the various species, see text and Tables 2 and 3.

(35) Glukhovtsev, M. N.; Bach, R. D.; Nagel, C. J. *J. Phys. Chem. A* **1997**, *101*, 316.

Table 3. Electronic States, Optimized Geometries, and Relative Energies[a] of Neutral and Anionic FeS_2 and Relevant Fragments Calculated at the B3LYP/6-311+G* Level of Theory[b]

	state	r_{Fe-S}, Å	r_{S-S}, Å	α_{SFeS}, deg	E_{rel}, eV
$Fe(S_2)$, **I**	$^5B_1$	2.20	2.22	60.6	0.18
	$^3B_2$	2.20	2.12	57.8	0.64
	$^1A_1$	2.11	2.07	58.8	2.08
SFeS, **II**	$^5B_2$	2.03	3.42	115.2	0.00
	$^3B_1$	2.02	3.42	116.1	0.27
	$^1A_1$	1.96	3.42	121.4	1.73
$SFeS^-$, **II**[c]	$^6A_1$	2.12	4.22	166.7	−3.30
	$^4\Pi$	2.14	4.28	180.0	−3.13
	$^2\Delta$	2.07	4.14	180.0	−2.46
$Fe + S_2$	$^5D/^3\Sigma^-$		1.93		2.13
$FeS + S$	$^5\Delta/^3P$	2.04			2.82[d]
$Fe + 2S$	$^5D/^3P$				6.16[d]
$Fe + S_2^-$	$^5D/^2\Pi$		1.93		0.33
$FeS + S^-$	$^5\Sigma/^2P$	2.12			0.62

[a] Energies at 0 K including ZPVE relative to SFeS ($^5B_2$). [b] All structures described are characterized as minima on the potential-energy surface by bearing only positive eigenvalues and three real vibrational frequencies. [c] Structure **I** is not considered further for the anion, because the vertical EA of $Fe(S_2)$ ($^5B_1$) is calculated as 1.71 eV. [d] These values combine to yield a computed $D_0(Fe-S)$ of 3.34 eV.

Scheme 2

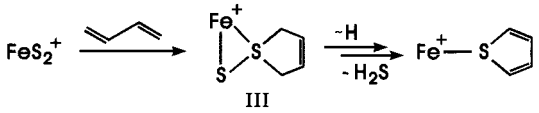

III

tackle this problem, in the present context it is sufficient to conclude that (i) structure **I** is favored and (ii) the high-energy isomer **II** easily rearranges to **I**.

Further, we briefly examined the neutral and anionic FeS_2 species with B3LYP/6-311+G* (Table 3). In accordance with previous suggestions,[4,5] a disulfide structure **II** is found for the anionic species. The computed adiabatic EA(SFeS) = 3.30 eV agrees quite well with the measured detachment energy of 3.28 eV[4] for FeS_2^-. The dichotomy between structures **I** and **II** is most pronounced for the neutral species, in which SFeS and $Fe(S_2)$ differ by no more than 0.18 eV. Considering the estimated accuracy of the theoretical level used, no definitive assignment of the most stable structure can be made. The computed data further predict IEs of 7.55 and 7.73 eV for the transitions $Fe(S_2) \rightarrow Fe(S_2)^+$ and $SFeS \rightarrow Fe(S_2)^+$ of the neutral structures, respectively. Both values are consistent with the experimental bracket of IE = 7.7 ± 0.5 eV derived above.

4. Discussion

The experimental and theoretical results confirm the suggestion of McMahon et al.[3] that FeS_2^+ exhibits structure **I**. However, the sulfur-atom transfer observed in some of the ion−molecule reactions described above may indicate occurrence of the rearrangement **I** → **II** upon approach of the reactants. Nevertheless, the considerable energy demand of structure **II** suggests an alternative mechanistic scenario. Specifically, S−S bond cleavage can also be rationalized if $Fe(S_2)^+$ can act as a thienoide in chemical reactions, in analogy to the oxenoide behavior of peroxides.[36] For example, loss of H_2S from the FeS_2^+/butadiene couple may be described in terms of Scheme 2 with formation of the multicentered structure **III** as the key step. This pathway circumvents the energetically demanding isomerization **I** → **II**.

(36) Boche, G.; Möbus, K.; Harms, K.; Lorenz, J. C. W.; Marsch, M. *Chem.—Eur. J.* **1996**, *2*, 604.

Scheme 3

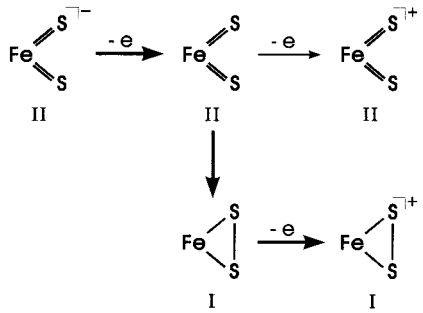

As far as thermochemistry is concerned, the preference of structure **I** also accounts for the increase from $D_0(Fe^+-S)$ = 3.08 ± 0.04 eV to $D_0(SFe^+-S)$ = 3.59 ± 0.12 eV upon ligation. An opposite trend is expected for structure **II** because the strengths of covalent metal−ligand bonds generally decrease with the formal oxidation state, i.e., formal Fe(III) in FeS^+ versus formal Fe(V) in $SFeS^+$.

The sector experiments also shed some light on the behavior of the neutral and anionic species. Thus, structure **II** is clearly preferred for the FeS_2^- anion,[5] whereas structure **I** is more favorable for cationic FeS_2^+. The comparative analysis of the $^-CR^+$ and $^-NR^+$ spectra of FeS_2^- implies an ambivalent situation for neutral FeS_2 in that both structures **I** and **II** appear feasible. The hypothesis of a unimolecular interconversion **II** → **I** for the neutral can also account for the increased yield of the recovery ion due to FeS_2^+ in the $^-NR^+$ spectrum of FeS_2^- compared to the $^-CR^+$ experiment, i.e., 28% versus 15% yield normalized to all ionic fragments. Thus, charge inversion of $SFeS^-$ in the $^-CR^+$ experiment mostly occurs in a single collision as a more or less vertical process leading to the unfavorable structure **II** for the resulting cation. Stepwise electron transfer in the $^-NR^+$ process does allow for partial rearrangement of the neutral species to structure **I** for which an enhanced reionization efficiency is expected. This situation is depicted in Scheme 3.

Obviously, this view of neutral FeS_2 is still very approximate and more detailed study of this structural dichotomy is indicated. For example, IE(FeS_2) = 7.7 ± 0.5 eV, determined in the bracketing experiments with FeS_2^+ described above, may refer to ionization of either neutral **I** or **II**, depending on the relative stability of these structures for the neutral as well as the possible interconversion with or without the reaction partner. Likewise, it may be the case that the experimentally determined threshold of 3.28 eV[4] for the electron detachment from FeS_2^- corresponds to the 0 → 0 transition $SFeS^- \rightarrow SFeS$, while the adiabatic EA may be lower if structure **I** is more stable than **II** for the neutral. In addition, the significantly different α_{SFeS} angles of the $SFeS^-$ anion and neutral SFeS may lead to unfavorable Franck−Condon factors for the 0 → 0 transition. In addition to these aspects concerning the experimental studies, the close spacings of the low-lying states of neutral and charged FeS_2 indicate that an inspection of this system using more sophisticated theoretical treatments than the B3LYP approach chosen here is warranted.

5. Conclusions

Sequential addition of sulfur to Fe^+ cation leads to the diatomic iron sulfide FeS^+ and then to $Fe(S_2)^+$ having the cyclic structure **I**. As a consequence of S−S bond formation in FeS_2^+, $D_0(SFe^+-S)$ = 3.59 ± 0.12 eV exceeds $D_0(Fe^+-S)$ = 3.08 ± 0.04 eV. Despite this strong bond, ion/molecule reactions can bring about sulfur-atom transfer from FeS_2^+ to various sub-

strates. Rather than involving an energetically demanding **I** → **II** rearrangement, structure **I** is suggested to act as a thienoide.[31] Fortunate circumstances allow the determination of $D_0(Fe^+-S) = 3.08 \pm 0.04$ eV with a high precision in two independent experiments. Hence, this particular diatomic system might be useful in benchmark calculations for evaluating the performance of contemporary theoretical methods. Last but not least, the present results indicate that the dichotomy between structures **I** and **II** is most pronounced for neutral FeS_2, and this system is certainly worthy of further experimental and theoretical studies.

Acknowledgment. Financial support by the Volkswagen-Stiftung, the Deutsche Forschungsgemeinschaft, the Fonds der Chemischen Industrie, and the National Science Foundation is acknowledged. We are grateful to the Konrad-Zuse-Zentrum Berlin for the generous allocation of computer time. Further, we thank Olaf Hübner for helpful comments.

Supporting Information Available: Computed vibrational frequencies and details of equilibrium measurements. This material is available free of charge via the Internet at http://pubs.acs.org.

IC990241B